Appalachian
STATE UNIVERSITY®
BOONE, NORTH CAROLINA

Flood Modeling in the Coastal Plains and Mountains: Analysis of Terrain Resolution

By: Jeffrey D. Colby

Abstract: The number of flood disasters has increased worldwide in recent decades. Identifying the optimal resolution or scale at which to represent digital terrain models (DTMs) is critical in order to improve our ability to accurately and efficiently model floods. Few studies have attempted to compare flood modeling results using different resolutions of DTMs in divergent environments. In this study flooding on the Tar River in the coastal plains and the Watauga River in the mountains of North Carolina were modeled using hydrologic information obtained following Hurricanes Floyd and Ivan. The effectiveness of DTMs derived from light detection and ranging and United States Geological Survey elevation data at commonly available resolutions in North Carolina were assessed. A quantitative diagnostic method based on measuring the distance flooded along transects was applied for evaluating the horizontal extent and internal pattern of flooding. The use of additional diagnostic metrics (area, volume, and shape) along with a visual graphic assessment enhanced the evaluation of flood modeling results. The extent and internal pattern of flooding in the low-relief coastal plains was found to be especially sensitive to the representation of terrain, and in the mountains 30 X 30-m data regardless of source were found to be dramatically unsuitable for flood modeling.

Flood Modeling in the Coastal Plains and Mountains: Analysis of Terrain Resolution

Jeffrey D. Colby and James G. Dobson

Introduction

The number of great flood disasters occurring worldwide has grown considerably over the last few decades (Todini 1999; Kundzewicz and Schellnhuber 2004). In the United States, for example, from the eastern coastal plains to the western mountains of North Carolina, flooding following Hurricanes Floyd in 1999 and Ivan in 2004 reached historic levels.

Determining the optimal representation of topography for flood modeling is critical (Hardy et al. 1999; Haile and Rientjes 2005). In one hydrologic study that was undertaken in diverse North Carolina watersheds including one in a forested wetland ecosystem near the coast and the other representing the southern Appalachian uplands, Sun et al. (2002) found that in both locations stormflow peaks and volume were most effected by topography. The influence of spatial scale effects on representing topography and predicting inundation is poorly understood (Horritt and Bates 2001). Although a few studies have compared the utility of digital terrain models (DTMs) at different spatial resolutions for flood modeling in lower relief areas (e.g., Horritt and Bates 2001; Omer et al. 2003; Raber et al. 2007), the writers are not aware of any studies of this type undertaken in mountain environments or studies comparing results from the coastal plains and mountains.

A number of studies have investigated the affects of digital terrain resolution on hydrologic modeling and simulations (e.g., Zhang and Montgomery 1994; Molnar and Julien 2000; Moglen and Hartman 2001), and drainage pattern extraction (Garbrecht and Martz 1994; Gyasi-Agyei et al. 1995). The key issues become how well does the resolution represent the features of the terrain and landscape, and at which resolution(s) do thresholds exist at which digital data can no longer accurately represent physical processes (Lam and Quattrochi 1992; Colby 2001).

According to Marcus et al. (2005), few researchers have evaluated the accuracy of variables such as basin, slope, network, and flow characteristics computed in mountain environments relative to low-relief areas and more research is clearly needed. Investigations undertaken separately in the two regions have underscored differences and similarities in regards to the influence of terrain representation and hydrologic character. Lowland area floodplain topography and hydrology are considered to be spatially and temporally complex (e.g., Stewart 1999; Hudson and Colditz 2003). Coastal floodplains are often portrayed as flat homogenous surfaces, however, topography strongly influences processes such as the duration and extent of flooding after recession of the flood crest (Hudson and Colditz 2003). Terrain characterization is often poorest where it is smoother, and large differences in values such as gradient can be generated from small elevation errors (Marcus et al. 2005). Where shallow floodplain gradients exist, flood inundation extent is affected by small changes in water surface elevations (Bates et al. 1997). According to Stewart (1999) high resolution representation of floodplain and river flow are required for flood modeling in lowland catchments.

The sources, as well as the spatial and temporal character of floods in mountain environments can differ significantly from

those occurring in the coastal plains. In addition to rainfall, flooding in mountainous areas may be due to rain on snowpack, snowmelt, and the failure of natural dams (Whol and Oguchi 2005). The dynamic hydrology of mountain environments is also spatially and temporally complex (Marcus et al. 2005). The rapid movement of precipitation into stream channels can be enhanced due to high relief, thin soils, intense (seasonal) precipitation, and sparse vegetation along with the close coupling of stream channels and hillslopes. In combination with elevation and aspect the distribution of these factors leads to high spatial variability in the frequency and magnitude of floods, making the prediction of flood extent and recurrence interval difficult in mountain environments (Whol and Oguchi 2005).

Evaluating terrain characterization in these two divergent environments raises questions such as: what is the optimal resolution or range of optimal resolutions for representing elevation data in each region, and are the optimal resolutions the same in both regions? If the optimal resolutions are different, what information is provided in terms of topographic characterization, and the hydrologic and hydraulic processes operating in the regions? Does the influence of data source override the effects of data resolution? It may seem straightforward to assume, for example, that DTMs derived from light detection and ranging (LIDAR) data are superior for flood modeling purposes compared to United States Geological Survey (USGS) digital elevation models (DEM). Using a simple DEM inundation method Wang and Zheng (2005), however, reported similarly accurate results in representing flooding extent in the coastal plains of North Carolina using 30×30-m LIDAR and 30×30-m USGS DEM data. Also, the resolution required by flood risk managers may be coarser than the finer spatial detail that can be supplied by geographic information system (GIS) databases (Zerger 2002; Zerger and Wealands 2004). Determining the utility of coarser resolution data could result in savings in terms of time, computational demands, data storage space, and human resources.

Representing terrain in digital form encourages the development of new methods for evaluating the accuracy of flood modeling results. Often it is assumed that if the vertical height of flood waters is modeled accurately the horizontal extent will also be accurate. However, the use of different DTMs will result in a difference in the horizontal boundaries of water surface profiles, and their implied intersection with the actual terrain surface. Less consideration has been given to determining the accuracy of the horizontal extent or pattern of flooding due in part to the difficulty in obtaining ground-truth information in order to verify the extent of flooding. Nevertheless, quantitative methods for determining the accuracy of the horizontal extent of flooding are needed (e.g., Wang and Zheng 2005). Additionally, elevation models vary in their representation of the terrain underneath floodwaters, which could lead to differences in flood volume calculations. Little information is available regarding acceptable ranges of error for flood modeling diagnostic metrics in divergent environments such as extent, area, shape, and volume.

The objective of this research study was to evaluate the utility of DEMs at commonly available resolutions for flood modeling in North Carolina, for reaches of the Tar River in the eastern coastal plains and the Watauga River in the western mountains. The North Carolina Floodplain Mapping Program (NCFMP) provides DEMs derived from LIDAR data for the state at 6.1×6.1 m (20×20 ft) and 15.2×15.2 m (50×50 ft) resolutions. The USGS provides 30×30 m (98.43×98.43 ft) resolution DEMs for the entire state. Descriptions and discussion are provided regarding the physical differences between the study areas,
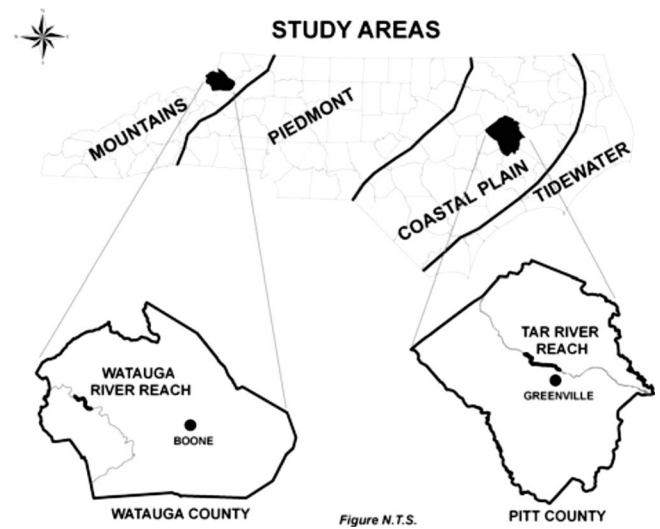

Fig. 1. Location of study area counties and river reaches in North Carolina

river reaches, their respective drainage basins, and flooding extents to provide a context for better understanding flood modeling results.

Study Areas

Tar River and Hurricane Floyd

Hurricane Dennis made landfall at Cape Hatteras, N.C. on September 4, 1999 producing 20–25 cm of rain east of Interstate 95. Hurricane Floyd followed on September 16, 1999, producing 25–50 cm of rain in less than 72 h in many areas of eastern North Carolina causing devastating flooding (e.g., Colby et al. 2000). Several sites on the Tar River downstream from Rocky Mount recorded recurrence intervals in excess of 500 years (Bales et al. 2000).

The reach of the Tar River modeled in this study was located near Greenville in the center of Pitt County within the coastal plains of eastern North Carolina (Fig. 1). Four large rivers systems, including the Tar/Pamlico River, drain the coastal plains which are characterized by broad flat floodplains to their north and somewhat steeper relief to the south. Near the city of Greenville the broad primary and secondary floodplains are occupied by open space and conservation land uses near the river with low and medium density residential, and mixed and industrial land uses extending northward (Colby et al. 2000). This area was chosen for study due to the extreme flooding that took place following Hurricane Floyd, the availability of a digital aerial photograph taken two days after peak flooding, and previous research experience with this reach of the river (e.g., Colby et al. 2000; Colby and Dobson 2006). The drainage area of the Tar River at Greenville was 6,889 km² (Table 1). The size of the study area, as defined by a roughly square area which encompassed the selected reach of the Tar River and its floodplain was 83.61 km². The elevation range of the study area was 25.44 m (maximum=25.06 m and minimum=−0.38 m), the mean elevation was 10.45 m, and the standard deviation was 6.28 m (based on a 6.1×6.1 m LIDAR-derived DEM). The mean slope value of the study area was 1.42°, and the gradient of the riverbed along this reach of the Tar River dropped approximately 1.06 m over 11.42 km (0.000093). Bales

Table 1. Comparative Physical Characteristics

Metrics	Tar River	Watauga River
Study area size	83.61 km^2	10.20 km^2
Elevation range	25.44 m	288.66 m
Elevation maximum	25.06 m	1,070.68 m
Elevation minimum	−0.38 m	782.02 m
Elevation mean	10.45 m	886.70 m
Elevation standard deviation	6.28 m	71.40 m
Slope mean	1.42º	18.7º
River reach length	11.42 km	3.54 km
Gradient	0.000093	0.0035
Daily average flow	82.2 m^3/s [a]	5.01 m^3/s
Peak Flow	1,850 m^3/s [a]	651 m^3/s
Drainage basin area	6,889 km^2 [a]	239 km^2
CSM—Daily flow	1.09[a]	1.92
CSM—Peak flow	24.51[a]	250
Average transect distance flooded	2,514.95 m	54.5 m
Area flooded/m of river reach	2,331 m^2/m	108 m^2/m

[a]Flow and drainage basin area measured at the Greenville gauge for calculating CSM.

et al. (2007) found a similar average bed slope over reach (0.00011) for an overlapping reach of the river. The discharge to drainage area ratio measured in cubic feet per second (ft^3/s) per square mile (CSM) calculated for the Tar River using daily mean flow was 1.09 (2,902 ft^3 s/2,660 mi^2), based on 9 years of data, 1998–2006, at the Greenville gauge, USGS (http://waterdata. usgs.gov/nwis/annual). Two days after peak flooding (September 23, 1999) the CSM calculated at the Greenville gauge was 24.51 (65,200 ft^3 s/2,660 mi^2).

Watauga River and Hurricane Ivan

Five years after Hurricane Floyd, unprecedented flooding affected the western part of the state. In September 2004, Hurricane Frances produced 15–50 cm of rain in the Appalachians and western North Carolina (National Climatic Data Center 2004). One week after Hurricane Frances, Hurricane Ivan arrived producing up to 30 cm of additional rain. The Watauga River experienced a 50-year recurrence interval flow event following Hurricane Ivan (USGS 2005), which was its second highest on record based on 66 years of data, with flooding extending beyond the 100-year floodplain in some areas.

The Watauga River originates on the western slopes of Grandfather Mountain, which is located in extreme northwestern North Carolina (Fig. 1). It generally flows north and west through Watauga County, the Watauga River Gorge, and eventually into Tennessee. Land classifications near the river in the study area consists of farmland (crops and pasture), forests (mixed timber), and areas of low density residential development. Steep banks and floodplain walls are found along the river. The reach of the river between the USGS gauge at Sugar Grove and the Hwy 321 Bridge was chosen for this study due to the significant flooding that occurred following Hurricane Ivan, the availability of discharge data at the upstream end of the study area, and accessibility for fieldwork. The drainage area of the Watauga River upstream from the Sugar Grove gauge was 239 km^2 (Table 1). The size of the study area, as defined by a roughly square area which encompassed the selected reach of the Watauga River and its floodplain was 10.20 km^2. The elevation range of the study area was 288.66 m (maximum=1,070.68 m and

minimum=782.02 m), the mean elevation was 886.70 m, and the standard deviation was 71.40 m (based on a 6.1×6.1 m LIDAR-derived DEM). The mean slope value of the study area was 18.7º, and the gradient of the riverbed along this reach of the Watauga River dropped approximately 12.5 m over 3.54 km (0.0035). The CSM for the Watauga River calculated using daily mean flow was 1.92 (177 ft^3 s/92 mi^2), based on 66 years of data, 1941–2006, at the Sugar Grove gauge, USGS (http:// waterdata.usgs.gov/nwis/annual). On September 17, 2004 (peak flow following Hurricane Ivan) the CSM for the Watauga River was 250 (23,000 ft^3 s/92 mi^2).

Methodology

The procedures and methods utilized in flood modeling for both the Tar and Watauga Rivers were conducted in a similar fashion with some differences which are discussed in the following sections. For each river reach, water surface profiles and depth grids were generated using triangulated irregular networks derived directly from LIDAR bare earth points and from a series of LIDAR (6.1×6.1, 15.2×15.2, and 30×30 m) and USGS (30×30 m) grid resolutions. The software used for this research included the Environmental Systems Research Institute (ESRI, Redlands, Calif.) ArcMap, and the HEC-RAS and HEC-GeoRAS United States Army Corp of Engineer (USACE 2002, 2005) programs. Quantitative diagnostic methods included comparisons of water surface profile extents and patterns based on (1) a statistical analysis of flooding distance along randomly spaced transects; (2) water surface profile areas; (3) depth grid volumes; and (4) the error in water surface polygonal area.

Data Acquisition

For the Tar River LIDAR bare earth data in the form of 3,048 m^2 (10,000 ft^2) tiles, were downloaded from the NCFMP website (http://www.ncfloodmaps.com). The LIDAR data for Pitt County were acquired in early 2001 during leaf-off conditions. Nine tiles of LIDAR bare earth data for the Tar River were obtained through the NCFMP. The LIDAR data for Watauga County were acquired in early 2003 during leaf-off conditions. Two tiles of LIDAR bare earth data for the Watauga River were obtained through the NCFMP. The nominal postspacing for the LIDAR data collected by the NCFMP averaged 4 meters across the state (http://www.eijournal.com/Floodplain_mapping.asp). The tiles in the form of **x**, **y**, and **z** vector data points were merged for each study area. The study area for the Tar River consisted of the nine tile area. The study area for the Watauga River was delineated using a bounding rectangle which encompassed the river reach and floodplain area. The merged LIDAR tiles for the Watauga River were clipped to the bounding rectangle to represent the study area. For the Tar River study area USGS national elevation dataset (NED) data (30×30 m) were originally downloaded from (http://edcwww.cr.usgs.gov/products/elevation/ned.html). Due to questions regarding NED data quality for the Watauga River study area, individual USGS quadrangles (30×30 m) were downloaded from the GIS Data Depot Web site (http:// data.geocomm.com/). The DEM quadrangles for the Watauga River were merged, and the USGS data were clipped to the respective study areas for each river. The USGS data for both study areas were DEM Level 2 data processed using a Linetrace contour-to-grid interpolation algorithm from digital line graph contours (Hodgson et al. 2003)

The vertical root-mean-square error (RMSE) for the LIDAR data collected in Pitt County was calculated by the NCFMP (http://www.ncgs.state.nc.us/floodmap.html) for the following categories: total (11.7 cm), grass (9.7 cm), weeds/crops (10.2 cm), scrub (13.5 cm), forest (13.5 cm), and built-up (10.5 cm). The USGS NED data in Pitt County had an RMSE of ±1 m. The RMSE for the LIDAR data collected in Watauga County was calculated by the NCFMP (http://www.ncgs.state.nc.us/floodmap.html) for the following categories: consolidated (23.2 cm), open terrain (11.9 cm), weeds/crops (16.5 cm), scrub (19.5 cm), forest (34.1 cm), and built-up (10.4 cm). The USGS DEM data in Watauga County had an RMSE of ±3.35 m.

Initial hydrologic parameters for the Tar River were obtained from the USGS gauge at Greenville located near the middle of the study area. The aerial photograph of flooding taken on September 23 was georeferenced using an image-to-image registration process with digital orthophoto quarter-quadrangles (DOQQs) from the area. For the Watauga River the USGS Sugar Grove gauge provided discharge measurements. An aerial photograph of flooding was not available for the Watauga River. Acquisition of remotely sensed data depicting flooding extents is difficult in mountain environments due to the flashy nature of the flood event, persistent cloud cover during peak flooding, and temporal constraints in terms of the timing of scheduled satellite overpasses or lead times required for requesting commercial satellite imagery or aerial photography (J. G. Dobson, unpublished MA thesis, 2006).

Elevation Data Preprocessing

In order to compare flood modeling results using elevation data from different sources and at a series of spatial resolutions, several preprocessing steps were undertaken to enable geometric data extraction from a commensurable data model. To implement the HEC-GeoRAS extension in ArcGIS the elevation data were required to be represented as a triangulated irregular network (TIN). In order to represent the LIDAR bare earth data at its original scale the data were converted directly to a TIN. The USGS 30×30 m gridded DEM data were also converted to a TIN. To test the LIDAR data at several resolutions (6.1×6.1, 15.2×15.2, and 30×30 m), the bare earth vector point data were first interpolated to raster grids using an inverse distance weighted (IDW) algorithm (number of points=12 and power=2). Other interpolation methods such as natural neighbor or kriging could be used to convert the LIDAR data to a grid, or alternative methods implemented to decimate the data and represent them at coarser scales (e.g., Omer et al. 2003; Raber et al. 2007). The IDW algorithm was used in this case due to the generally even and dense sampling of points and because IDW is a commonly used method for generating DEMs (e.g., Gueudet et al. 2004; Lloyd and Atkinson 2006). The 6.1×6.1 m (20×20 ft) and 15.2×15.2 m (50×50 ft) resolutions were chosen to match the resolution of gridded LIDAR data available from the NCFMP. The LIDAR-derived DEMs were not fully hydrologically corrected as are the 15.2×15.2 m DEMs available from the NCFMP. A comparison of similarly processed DTMs was sought in this study, and the NCFMP has removed data points from the bare earth LIDAR data that represent obstructions such as bridges, which provides a level of hydrologic correction. These grids were then converted to TINs. This interpolation and conversion method enabled a comparison of results from the LIDAR and USGS data using the same data model format.

Table 2. Tar River Calibration Values

Discharge (m³/s)	Water surface level (m)	Manning's roughness coefficients
1,850[a]	8.34[a]	0.035, 0.144, and 0.192 (20% ↑)
1,770 (4% ↓)	7.51(10% ↓)	**0.035, 0.12,** and **0.16**[a]
1,660 (10% ↓)	7.09 (15% ↓)	0.035, 0.096, and 0.128, (20% ↓)
	6.92 (17% ↓)	
	6.67 (20% ↓)	
	6.26 (25% ↓)	

[a]Initial values, values in bold used for modeling.

Flood Modeling

There were essentially three phases to the flood modeling process. The process was based on first implementing the hydraulic extension program HEC-GeoRAS within ArcGIS. Using HEC-GeoRAS a geometric data file was created consisting of a stream centerline, left and right banks, left and right flowpaths, and cross-section cut lines. A geometric data file was generated from each terrain resolution resulting in five files for each river (i.e., from LIDAR bare earth, LIDAR 6.1×6.1-m, LIDAR 15.2×15.2-m, LIDAR 30×30-m, and USGS 30×30-m elevation data).

In the second phase of the process the geometric data files were imported into the HEC-RAS hydraulic model. For the Tar River estimates were entered for daily mean discharge, daily mean water surface level, and Manning's roughness coefficients. For the Watauga River estimates were entered for peak discharge, peak water surface level, and Manning's roughness coefficients. A steady and subcritical flow analysis was used to generate water surface profiles for both rivers.

The third modeling phase entailed exporting the water surface profiles from HEC-RAS back into ArcGIS through HEC-GeoRAS. A parameter specified during the export process was the grid resolution at which to represent the water surface profiles and depth grid. For the LIDAR bare earth data the grid resolutions were determined based on the following equation (Tobler 1988; Moglen and Hartman 2001)

$$d = \sqrt{\frac{A}{n}} \qquad (1)$$

where d=average horizontal resolution; A=mapped area; and n=number of point measurements. The calculated resolutions for the Tar and Watauga River data were 5.8×5.8 m and 5.2×5.2 m, respectively. These resolutions were then rounded to the 6.1×6.1 m (20×20 ft) resolution.

Model Calibration

Calibration for the water surface profiles generated using HEC-RAS was undertaken using the geometric data file extracted from the TIN derived from the LIDAR bare earth data for both study areas. Initial values for discharge and water surface level for the Tar River were estimated based on a relationship between drainage area calculated for the upper and lower ends of the study area and distance from the USGS gauge at Greenville (e.g., Colby et al. 2000; Bales et al. 2007). Hydrologic values for the USGS gauge at Greenville were obtained for the date the aerial photograph of flooding was taken. A series of water surface profiles were generated through systematic testing of a range of discharge, water surface levels, and Manning's roughness coefficient esti-

Table 3. Watauga River Manning's *n* Values

Manning's roughness coefficients
0.05, 0.052, and 0.1425 (50% ↑)
0.05, 0.049, and 0.133 (40% ↑)
0.05, 0.0455, and 0.1235 (30% ↑)
0.05, 0.042, and 0.114 (20% ↑)
0.05, 0.0385, and 0.1045 (10% ↑)
0.05, 0.035, and **0.095**[a]
0.05, 0.0315, and 0.0855 (10% ↓)
0.05, 0.028, and 0.076 (20% ↓)
0.05, 0.0245, and 0.0665 (30% ↓)
0.05, 0.021, and 0.057 (40% ↓)
0.05, 0.0175, 0.0475 (50% ↓)

[a]Initial values, values in bold used for modeling.

mates (Table 2). The water surface profiles generated through this process were overlaid on the aerial photograph of flooding and visual assessment determined how well the profiles represented the extent of flooding. James and Burgess (1982) noted that criterion for evaluating successful calibration may include subjective judgment or some statistic measuring goodness of fit. For the Tar River a measurement of the mean percentage of transects flooded which extended across the water surface profiles (described below), also supported the final selection of calibration parameters.

For the Watauga River less calibration effort was required since the peak discharge value was obtained from the Sugar Grove gauge. Water surface level was estimated based on in situ photographs taken near peak flood stage. A range of water surface level values were tested and the initial estimate retained. Global positioning system coordinate points of high water marks, represented by debris lines and acquired soon after the flood by the writers, were overlaid on the water surface profiles and visual assessment determined how well the profiles represented the extent of flooding according to the high water marks. Assessments of water surface profile boundaries were also based on in situ photographs taken at various locations near peak flood stage.

The calibration process, such as the selection of roughness coefficients, could mask effects of scale. However, Horritt and Bates (2001) found that the influence on inundation extent of optimal Manning's roughness coefficients were constant with respect to changes in scale. Pappenberger et al. (2005) noted finding a stable combination of roughness values can be very difficult, and typically one value for the channel and floodplain are used (Horritt and Bates 2001). Manning's roughness coefficients were estimated for each river from 1998 color infrared DOQQs and personal site visits soon after the flood events. For the Watauga River, a range of ±50% of the original Manning's roughness coefficient estimates at intervals of 10% were tested, and the original values retained (Table 3) (J. G. Dobson, unpublished MA thesis, 2006). Following calibration, water surface profiles for both rivers were generated using the geometric data files produced using the LIDAR 6.1×6.1, 15.2×15.2, and 30×30-m, and USGS 30×30-m data.

Diagnostics

Several diagnostic methods were used to evaluate flood modeling results. A diagnostic method was applied to evaluate the accuracy of the horizontal extent and internal pattern of the water surface profiles using 34 randomly spaced transect lines, and calculating a
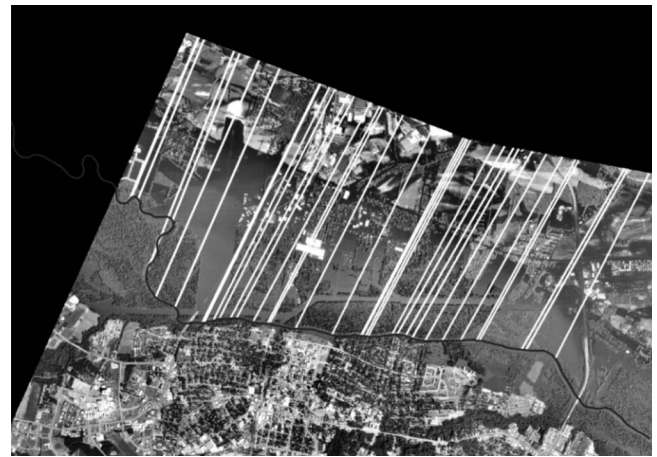

Fig. 2. Tar River aerial photograph of flooding overlaid with diagnostic transects

statistical comparison of the distance flooded measured along the transects. The digital shoreline analysis system (DSAS) developed by the USGS computes rate-of-change statistics for boundary changes from clearly identified positions using transects (Thieler et. al 2005), and other similar programs may exist. However, the writers are not aware of the application of the DSAS or similar programs to evaluating changes in the horizontal extent and internal pattern of water surface profiles.

For the Tar River the lengths of the transects were limited to the extent of the aerial photograph taken two days after peak flooding, since the photograph represented the extent of ground-truth information (Fig. 2). Inspection of the water surface profiles generated from the series of DTMs indicated little difference in the extent and pattern of flooding on the south side of the river due to higher relief in this area and a narrow floodplain along a significant distance of the river reach. The water surface profiles displayed considerable differences in the extent and pattern of flooding in the broad flat floodplain to the north of the river. The transects for the Tar River were drawn to the north of the river in order to focus on detecting differences in the utility of different DTM resolutions for flood modeling in the most extensive and sensitive area of the floodplain. The transects were drawn approximately parallel to each other. Due to meanders in the river attempting to draw the transects perpendicular to the stream channel may have resulted in some long transects running approximately parallel to the river. Due to the more symmetric nature of the terrain and extent of flooding on both sides of the Watauga River, the 34 randomly spaced transect lines were drawn on alternating sides of the river and perpendicular to the stream channel (Fig. 3).

The water surface profiles were intersected with the transect lines in order to calculate the distance flooded along each transect (Fig. 4). Distances encountered along a transect line that were not flooded (e.g., islands) were not included in the flooded distance measurement. It was important not to include areas of emergent terrain that were not flooded in order to detect differences in the internal pattern of flooding.

One calibration metric used for the Tar River using the transects was the mean percentage of transects flooded. This metric was calculated by dividing the distance flooded along a transect by the transect length, and calculating the mean value for the set of transects. For the Tar River the mean percentage of the transect distances flooded on the water surface profile generated

**Fig. 3.** Watauga River infrared DOQQs (1998) overlaid with diagnostic transects

from the LIDAR bare earth data (79%) was the same as that measured on the aerial photograph (79%), which provided descriptive statistical information to support the effective calibration of the water surface profile.

In order to perform inferential statistical analysis of the transect distances flooded, the measurements for the water surface profiles for each river were tested for normality, and were found not to be normally distributed. Log transformations were performed resulting in normalized data for the Watauga River but not for the Tar River. In order to determine whether statistically significant differences existed between the flooded distance measurements a nonparametric Sign test was performed on the Tar River data, and a comparable parametric Paired-T test was performed on the Watauga River data. For the Tar River the sets of flooded distance measurements were compared to the flooded distances measured along the transects overlaid on the aerial photograph. For the Watauga River the sets of flooded distance measurements were compared to the distances measured along the transects overlaid on the LIDAR bare earth 6.1×6.1 m water surface profile. The null hypothesis for the tests was that there was no difference between the sets of flooded distance measurements. At the 0.05 alpha (significance) level, a p-value (asymptotic significance value) less than 0.05 indicated that the null hypothesis should be rejected.

The area of the water surface profiles and the volume calculations of the depth grids were calculated in ArcMap. The water surface profile feature class is created from the geometry of the depth grid with an attribute table containing a shape area calculation. The volume measurement represents the amount of cubic space below a reference plane and was calculated using the 3-D Analyst extension. Volume calculations using LIDAR DTMs did not include the depth of the river channel that was covered with water at the time of data acquisition.

Evaluation of the overall shape and area of the water surface profiles was undertaken based on a symmetric difference comparison with the water surface profile derived from the highest resolution data using an error in water surface polygonal area calculation (after Gueudot et al. 2004)

$$\text{Error}(\%) = \frac{\text{Area(Poly)} + \text{Area(REFPoly)} - 2x\text{Area(Poly} \cap \text{REFPoly})}{\text{Area(REFPoly)}} \times 100 \quad (2)$$
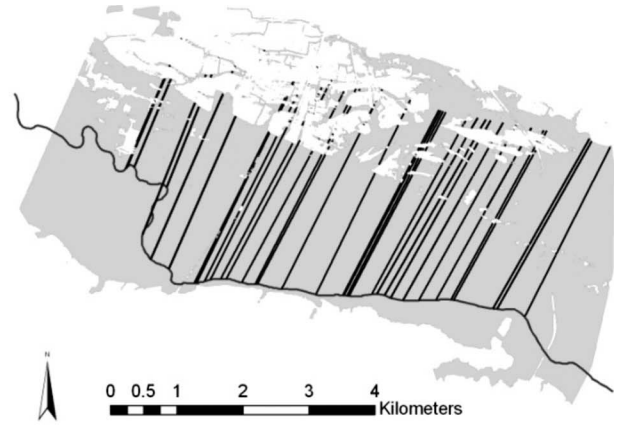
a).
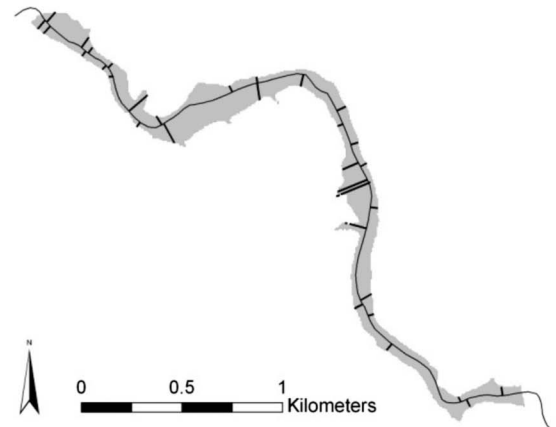
b).

Fig. 4. Example water surface profiles overlaid with intersected diagnostic transects: (a) Tar River; (b) Watauga River

where Poly refers to the polygon of the water surface profile being evaluated and REFPoly refers to the reference polygon (LIDAR bare earth 6.1×6.1 m). Similar types of comparisons have been made for linear features using buffers (Goodchild and Hunter 1997; Hodgson et al. 2004). A modified version of the two buffer method introduced by Hodgson et al. (2004), was used to calculate a feature agreement statistic for comparison of water surface profile polygons by Raber et al. (2007). As discussed by Raber et al. (2007) this type of feature agreement statistic is more appropriately applied towards comparisons of water surface profiles generated from the same river reach.

Results

Diagnostic results for the Tar and Watauga Rivers are provided in Tables 4 and 5, respectively. The results of the Sign test for the Tar River indicated that distances flooded along the transects on the water surface profiles generated from the LIDAR 15.2×15.2-m, LIDAR 30×30-m, and USGS 30×30-m data were statistically significantly different from the distances flooded along the transects on the aerial photograph (Table 4). The area and volume results for the Tar River derived from the LIDAR data sets (6.1×6.1, 15.2×15.2, and 30×30 m) were

Table 4. Diagnostic Results for the Tar River

Profile resolution (m²)	Sign test p-value w/aerial photo	Inundated area (m²)	Area percent difference w/LIDAR bare earth 6.1×6.1 m	Inundated volume (m³)	Volume percent difference w/LIDAR bare earth 6.1×6.1 m	Percent error in water surface polygonal area
LIDAR bare earth 6.1	0.864	26,624,376		76,739,289		
LIDAR 6.1	0.123	27,029,619	2	77,513,201	1	2.24
LIDAR 15.2	0.010[a]	27,298,861	3	77,985,179	2	5.21
LIDAR 30	0.026[a]	27,250,818	2	76,886,104	0	5.41
USGS 30	0.040[a]	29,090,619	9	85,957,167	11	12.85
Aerial photo						

[a]Significant at alpha=0.05.

within 3% compared to the LIDAR bare earth 6.1×6.1-m results. The water surface profile and depth grid generated using the USGS 30×30-m data overestimated both area and volume (9% and 11%, respectively). The error in water surface polygonal area diagnostic values generated using the LIDAR data sets increased from 6.1×6.1 m (2.24%) to 15.2×15.2 m (5.21%) with similar values for the 15.2×15.2 and 30×30-m resolutions. The error provided by the USGS 30×30-m data was 12.85%.

For the Watauga River the results of the Paired-T test indicated that distances flooded along the transects only on the water surface profile generated from the USGS 30×30-m data were statistically significantly different from the LIDAR bare earth 6.1×6.1-m water surface profile (Table 5). The area and volume results for the Watauga River derived from the LIDAR data sets (6.1×6.1, 15.2×15.2, and 30×30 m) were within 5% compared to the LIDAR bare earth 6.1×6.1-m results, except for the volume measurement derived from the LIDAR 30×30-m data which was 33% lower. The area and volume measurements for the USGS 30×30-m data were notably high. The results of the error in water surface polygonal area diagnostic indicated a more evenly increasing trend compared to the Tar River, although, the overall values were generally higher for the Watauga River, with the best fit provided by the water surface profile derived from the LIDAR 6.1×6.1-m data.

A review of their physical characteristics illustrates fundamental differences between the rivers' study areas, selected river reaches, and drainage basins, and can help inform an evaluation of flood modeling results. For example, the topographic character of the study areas (e.g., mean slope: Tar=1.42° and Watauga=18.7°), gradients of the river reaches (Tar=0.000093 and Watauga=0.0035) and size of the drainage areas (Tar=6,889 km² and Watauga=239 km²) were clearly different (Table 1). The CSM ratio (discharge to drainage area) enables valid comparison between runoff from different size watersheds (Black 1996). CSM values tend to be lower for larger and flatter basins, and higher for small, hilly, rocky, or urban basins (Buckelew 1998). The CSM values based on daily mean flow were 1.09 for the Tar River and 1.92 for the Watauga River. At maximum flow the CSM ratios were 24.51 and 250 for the Tar and Watauga Rivers, respectively. These daily and maximum flow CSM values were similar to those calculated for comparable drainage basins in the United States (Patrick 1994). Additionally, the average transect distance flooded (Tar=2,514.95 m and Watauga=54.5 m) enables comparisons between the extent of flooding in the two study areas and their topographic character (Table 1). It should be noted that transects for the Tar River were drawn to the north of the river to cover the greatest extent of flooding. The overall greater extent of flooding along the Tar River was evident in the total area flooded, which was 70 times larger based on the LIDAR bare earth 6.1×6.1-m water surface profiles (Tables 4 and 5). A normalized comparison can be made by calculating the area flooded per meter of river reach. For the Tar River this figure was 2,331 m²/m and for the Watauga River it was 108 m²/m (Table 1). Comparison of the last three metrics illustrates the much greater spatial extent of flooding in the coastal plains than in the mountains.

Discussion

In regards to the inferential statistical analysis, the Tar River results from the Sign test indicated a significant difference in the extent and pattern of flooding when using data at coarser resolutions than 6.1×6.1 m. The differences in the area, volume, and error in water surface polygonal area values from using the LIDAR data seemed small and may have been attenuated by the size of the area flooded. However, small differences in area and volume represented substantial amounts when considering the total extent of flooding. With the statistically significant results of

Table 5. Diagnostic Results for the Watauga River

Profile resolution (m²)	Paired-T p-value w/LIDAR bare earth 6.1×6.1 m	Inundated area (m²)	Area percent difference w/LIDAR bare earth 6.1×6.1 m	Inundated volume (m³)	Volume percent difference w/LIDAR bare earth 6.1×6.1 m	Percent error in water surface polygonal area
LIDAR bare earth 6.1		382,909		1,301,706		
LIDAR 6.1	0.356	394,504	3	1,337,187	3	6.74
LIDAR 15.2	0.518	402,502	5	1,279,401	−2	12.42
LIDAR 30	0.269	374,741	−2	873,603	−33	23.89
USGS 30	0.033[a]	453,258	18	1,616,399	24	36.82

[a]Significant at alpha=0.05.

the Sign test, and a 5% error in water surface polygonal area measurement the results derived from the 15.2×15.2 m should be questioned for this river reach. Interestingly, the diagnostic results from using the LIDAR 30×30-m data were similar to that obtained from using the LIDAR 15.2×15.2-m data. Another point to consider is that the p-values from the Sign test were lower for the water surface profiles generated from the gridded data. Comparison of the p-values for the LIDAR bare earth 6.1×6.1 m and the LIDAR 6.1×6.1-m water surface profiles suggests that the preprocessing method selected to construct a DTM from LIDAR data may influence flood modeling results.

For the Watauga River the p-values from the Paired-T test indicated a significant difference in the extent and pattern of flooding only when using the USGS 30×30-m data. For the Watauga River the p-values from the Paired-T test were generally higher than the p-values from the Sign test for the same data resolutions for the Tar River. These higher values may be indicative of a similar extent and pattern of flooding. In the mountains, as discharge increases flood waters may rise up the valley walls rather than extending outward as occurs in the coastal plains, resulting in a similar internal pattern of flooding (e.g., without islands or emergent areas of terrain in the floodplain).

For the Watauga River the Paired-T test compared the extent of water surface profiles at coarser resolutions with that generated using the finest scale data (i.e., the LIDAR bare earth 6.1 ×6.1-m data) rather than with an aerial photograph of flooding. To further explore the implications of this comparison, a Sign test was conducted for the Tar River comparing the water surface profiles generated from coarser resolution data with that derived from the LIDAR bare earth 6.1×6.1-m data. In contrast to the values obtained for the Watauga River, the values for the Tar River water surface profiles were all statistically significantly different, which supported the idea that the extent and internal pattern of flooding in the mountains represented at different resolutions was more similar than that found in the coastal plains.

Even with a less intricate pattern of flooding, the error in water surface polygonal area values calculated for the water surface profiles derived from the LIDAR data for the Watauga River were higher than those for the Tar River, which was attributed to the size of the areas flooded along the two rivers. Compared to the attenuating effect of the large area flooded along the Tar River, when this diagnostic metric was calculated for the Watauga River, reasonably differentiating results were obtained. This interpretation is supported by the slightly more variable surface area measurements obtained for the Watauga River (Table 5). Although, the extent and internal pattern of flooding at 15.2×15.2 m was not statistically different from the results obtained using the LIDAR bare earth 6.1×6.1-m data, the area difference (5%) and error in water surface polygonal area measurements (12.42%) could raise questions regarding the utility of this resolution.

Two related studies support the findings of this research (Omer et al. 2003; Raber et al. 2007). Using an angular filtering method, Omer et al. (2003), decimated original LIDAR data points (to 1º, 2º, 4º, 8º, and 12º) collected for a study area located in the Piedmont region of North Carolina (Fig. 1). The 2.3 mi² Lieth Creek study area had a 0.001 slope gradient. An estimated equivalent horizontal resolution for the number of points resulting from each degree of filtering can be calculated using Eq. (1). The writers found that cross section analyses, hydraulic modeling results (water surface elevation), and floodplain delineation (flood areas) remained uncompromised using LIDAR data filtered to 4º (approximately 9.5×9.5 m).

Raber et al. (2007), also working in the Piedmont of North

Carolina along the 5-km Reedy Fork Creek, evaluated the accuracy of base flood elevations and flood zone boundaries through a sensitivity study using TINs derived from LIDAR data decimated from a reference dataset to a series of simulated postspacings (i.e., 2.10, 4.12, 6.28, 8.50, and 10.80 m). They found no pattern of error in DEM (TIN) accuracy, and base flood elevations did not statistically change over the postspacing values tested. Flood zone boundaries, however, were found to be sensitive to postspacing variations. The writers suggested that the positions of the flood zone boundaries were likely due to surface form accuracy rather than absolute vertical accuracy. Their overall results indicated that collecting LIDAR data at less than 4 m (equivalent postspacing of 4.12–6.28 m) may not be justified.

Volume measurements calculated from the respective depth grids provided additional insight into the selection of data source and resolution. Differences in volume measurements for the Tar River were lower than for the Watauga River, primarily due to the lack of relief in the coastal plains. For the Watauga River the volume measurements from the LIDAR 30×30 m and the USGS 30×30-m data were considerably different from the volume measurement calculated from the LIDAR bare earth 6.1×6.1-m data (Table 5). An assessment of water surface profiles generated from the LIDAR bare earth, LIDAR 30×30 m, and USGS 30×30-m data draped over their respective TINs and 15×15-cm aerial photography for the Watauga River provide a visual source of information for better understanding the difference in volume and area measurements [Figs. 5(a–c)].

Inspection of the water surface profiles generated from the 30×30-m data revealed discrepancies in their extent, shape, and location. In both Figs. 5(b and c), larger serrated edges are evident due to the coarser resolution of the terrain models from which the profiles were generated compared with the water surface profile derived from the LIDAR bare earth 6.1×6.1-m data [Fig. 5(a)]. In Fig. 5(c), however, the serrated edge of the USGS 30×30-m water surface profile is offset farther to the right of the river and appears to climb the terrain, when compared to that of the LIDAR 30×30-m profile. The gaps in the serrated edge of the LIDAR 30×30-m profile as well as its overall shorter width along the river channel likely contributed to the lower volume measurements. The extended water surface profile at the center left of the river likely did not contribute to a significant increase in volume due to the shallow depth in that area.

Additionally, the coarser resolution of the LIDAR 30×30-m grid cells did not capture the character of the approximately 25-m wide channel (Horritt and Bates 2001; Haile and Rientjes 2005). Previous research has found that terrain represented at coarser resolutions had difficulty in representing river meanders and depth in the outer meander bends (Hardy et al. 1999; Moglen and Hartman 2001). This lack of accurate channel characterization is also true for the USGS 30×30-m data, however, poor representation of the floodplain resulted in greater volume and area calculations.

Conclusions

The findings from this research along the Tar River suggest that flood modeling using high resolution representation of terrain is needed to better represent flooding extent in lowland coastal plains regions. Although, the LIDAR 30×30-m data provided similar results as the LIDAR 15.2×15.2-m data, a representation of the terrain based on the USGS 30×30-m data was found to be less useful. For the Watauga River somewhat different results

Fig. 5. Water surface profiles overlaid on respective TINs and 15 ×15 cm aerial photography: (a) LIDAR bare earth 6.1×6.1 m; (b) LIDAR 30×30 m; and (c) USGS 30×30 m

were obtained. As in the coastal plains the LIDAR 6.1×6.1-m data provided better overall results. LIDAR data represented at 15.2×15.2-m resolution may be useful in the mountains, however, due to the steeper terrain and more limited horizontal extent of flooding. However, depending upon application, questions of utility could arise based on the percent differences for the inundated area and the error in water surface polygonal area at the 15.2×15.2-m resolution. Terrain characterizations at the 30×30-m resolution were found to be dramatically unsuitable for flood modeling in this mountainous area, regardless of data source.

Terrain can be considered a filter through which to answer questions such as, which factor was more influential on flood modeling results, data source or resolution? In the low-relief coastal plains the USGS data did not perform as well as similar resolution LIDAR data. With the greater topographic relief in the mountains and the narrower channel of the Watauga River, 30×30-m data regardless of source could not sufficiently capture the character of the terrain.

With the findings of Raber et al. (2007) which indicated that

acquisition of LIDAR data is unnecessary at a finer postspacing than is already standard for the NCFMP (4 m), further study could be focused on evaluating a finer series of coarser DTM resolutions. The series of resolutions should include 10×10 m which falls between the resolutions which worked well (6.1×6.1 m) and could be questioned (15.2×15.2 m) in this study, and which may be useful according to other studies (Zhang and Montgomery 1994; Omer et al. 2003). Additional further research could include evaluating methods for converting bare earth LIDAR data to DTMs for flood modeling, and the development of complexity metrics (e.g., Woolard and Colby 2002) for assessing the surface form of DTMs for flood modeling purposes. The comparative metrics calculated for the study areas, river reaches, drainage basins, and flooding extents (including area per meter of river reach) in this paper can be compared to characteristics in other regions, and provide a context for better understanding flood modeling results in divergent environments.

References

Bales, J. D., Oblinger, C. J., and Sallenger, A. H., Jr. (2000). "Two months of flooding in eastern North Carolina, September–October 1999: Hydrologic, water quality, and geologic effects of Hurricanes Dennis, Floyd, and Irene." *U.S. Geological Survey Water-Resources Investigations Rep. No. 00-4093*, U.S. Geological Survey, Denver.

Bales, J. D., Wagner, C. R., Tighe, K. C., and Terziotti, S. (2007). "LiDAR-derived flood-inundation maps for real-time flood-mapping applications, Tar River Basin, North Carolina." *U.S. Geological Survey Scientific Investigations Rep. No. 2007-5032*, U.S. Geological Survey, Reston, Va.

Bates, P. D., Horritt, M. S., Smith, C. N., and Mason, D. (1997). "Integrating remote sensing observations of flood hydrology and hydraulic modeling." *Hydrolog. Process.*, 11(14), 1777–1795.

Black, P. E. (1996). *Watershed hydrology*, Ann Arbor, Chelsea, Mich.

Buckelew, T. (1998). "CSM: A unit of measurement for interpreting hydrologic data." ⟨http://www.erh.noaa.gov/nerfc/csmpaper.htm⟩ (Jan. 15, 2008).

Colby, J. D. (2001). "Simulation of a Costa Rican watershed: Resolution effects and fractals." *J. Water Resour. Plann. Manage.*, 127(4), 261–270.

Colby, J. D., and Dobson, J. G. (2006). "Flood modeling in the coastal plains and mountains." *Proc., 2006 American Water Resources Association Spring Specialty Conf. on GIS and Water Resources IV*, AWRA, Houston, Tex.

Colby, J. D., Mulcahy, K. A., and Wang, Y. (2000). "Modeling flooding extent from Hurricane Floyd in the coastal plains of North Carolina." *Global Environmental Change Part B: Environmental Hazards*, 2(4), 157–168.

Garbrecht, J., and Martz, L. (1994). "Grid size dependency of parameters extracted from digital elevation models." *Comput. Geosci.*, 20(1), 85–87.

Goodchild, M. F., and Hunter, G. J. (1997). "A simple positional accuracy measure for linear features." *Int. J. Geogr. Inf. Syst.*, 11(3), 299–306.

Gueudet, P., Wells, G., Maidment, D., and Neuenschwander, A. (2004). "Influence of the post-spacing of the LIDAR-derived DEM on flood modeling." *Proc., 2004 American Water Resources Association Spring Specialty Conf., GIS and Water Resources III*, AWRA, Nashville, Tenn.

Gyasi-Agyei, Y., Willgoose, G., and De Troch, F. P. (1995). "Effects of vertical resolution and map scale of digital elevation models on geomorphological parameters used in hydrology." *Hydrolog. Process.*, 9(3–4), 363–382.

Haile, A. T., and Rientjes, T. H. M. (2005). "Effects of LIDAR resolution in flood modeling: A model sensitivity study for the city of Tegucigalpa, Honduras." *Proc., 36th Int. Society for Photogrammetry and Remote Sensing Conf., Laser Scanning Workshop*, ISPR, Enschede, The Netherlands.

Hardy, R. J., Bates, P. D., and Anderson, M. G. (1999). "The importance of spatial resolution in hydraulic models for floodplain environments." *J. Hydrol.*, 216(1–2), 124–136.

Hodgson, M. E., et al. (2003). "An evaluation of LIDAR-derived elevation and terrain slope in leaf-off conditions." *Photogramm. Eng. Remote Sens.*, 71(7), 817–823.

Hodgson, M. E., Li, X., and Cheng, Y. (2004). "A parameterization model for transportation feature extraction." *Photogramm. Eng. Remote Sens.*, 70(12), 1399–1404.

Horritt, M. S., and Bates, P. D. (2001). "Effects of spatial resolution on a raster based model of flood flow." *J. Hydrol.*, 253(1–4), 239–249.

Hudson, P. F., and Colditz, R. (2003). "Flood delineation in a large and complex alluvial valley: The lower Pánuco Basin, Mexico." *J. Hydrol.*, 280(1–4), 229–245.

James, L. D., and Burgess, S. J. (1982). "Selection, calibration, and testing of hydrologic models." *Hydrologic modeling of small watersheds*, ASAE, St. Joseph, Mich., 409–434.

Kundzewicz, Z. M., and Schellnhuber, H. J. (2004). "Floods in the IPCC tar perspective." *Natural Hazards*, 31(1), 111–128.

Lam, N. S., and Quattrochi, D. A. (1992). "On the issues of scale, resolution, and fractal analysis in the mapping sciences." *Profess. Geograph.*, 44(1), 88–98.

Lloyd, C. D., and Atkinson, P. M. (2006). "Deriving ground surface digital elevation models from LIDAR data with geostatistics." *Int. J. Geograph. Inf. Sci.*, 20(5), 535–563.

Marcus, W. A., Aspinall, R. J., and Marston, R. A. (2005). "Geographic information systems and surface hydrology in mountains." *Geographic information science and mountain geomorphology*, M. P. Bishop and J. F. Shroder Jr., eds., Springer, New York, 343–379.

Moglen, G. E., and Hartman, G. L. (2001). "Resolution effects on hydrologic modeling parameters and peak discharge." *J. Hydrol. Eng.*, 6(6), 490–497.

Molnar, D. K., and Julien, P. Y. (2000). "Grid-size effects on surface runoff modeling." *J. Hydrol. Eng.*, 5(1), 8–16.

National Climatic Data Center. (2004). "Climate of 2004 Atlantic hurricane season." ⟨http://www.ncdc.noaa.gov/oa/climate/research/2004/sep/frances-rainfall.txt⟩ (Dec. 5, 2004).

Omer, C. R., Nelson, E. J., and Zundel, A. K. (2003). "Impact of varied data resolution on hydraulic modeling and floodplain delineation." *J. Am. Water Resour. Assoc.*, 39(2), 467–475.

Pappenberger, F., Beven, K., Horritt, M., and Blazkova, S. (2005). "Uncertainty in the calibration of effective roughness parameters in HEC-RAS using inundation and downstream level observations." *J. Hydrol.*, 302(1–4), 46–69.

Patrick, R. (1994). *Rivers of the United States: Chemical and physical characteristics*, Vol. II, Wiley, New York.

Raber, G. T., Jensen, J. R., Hodgson, M. E., Tullis, J. A., Davis, B. A., and Berglund, J. (2007). "Impact of LIDAR nominal post-spacing on DEM accuracy and flood zone delineation." *Photogramm. Eng. Remote Sens.*, 73(7), 793–804.

Stewart, M. D., Bates, P. D., Anderson, M. G., Price, D. A., and Burt, T. P. (1999). "Modeling floods in hydrologically complex lowland river reaches." *J. Hydrol.*, 223(1–2), 85–106.

Sun, G., et al. (2002). "A comparison of the watershed hydrology of coastal forested wetlands and the mountainous uplands in the southern U.S." *J. Hydrol.*, 263(1–4), 92–104.

Thieler, E. R., Himmelstoss, E. A., Zichichi, J. L., and Miller, T. L. (2005). "Digital shoreline analysis system (DSAS) version 3.0: An ArcGIS© extension for calculating shoreline change." *U.S. Geological Survey Open-File Rep. No. 2005-1304*, U.S. Geological Survey, Woods Hole, Mass.

Tobler, W. R. (1988). "Resolution, resampling, and all that." *Building Databases for Global Science: Proc., 1st Meeting of the Int. Geographical Union Global Database Planning Project*, H. Mounsey and R. F. Tomlinson, eds., Taylor and Francis, London, 129–137.

Todini, E. (1999). "An operational decision support system for flood risk mapping, forecasting, and management." *Urban Water*, 1(2), 131–143.

United States Army Corps of Engineers (USACE). (2002). *HEC-RAS river analysis system version 3.1.2 users manual*, Hydrologic Engineering Center, Davis, Calif.

United States Army Corps of Engineers (USACE). (2005). *HEC-GeoRAS, GIS tools for HEC-RAS using ArcGIS, Version 4.0 users manual*, Hydrologic Engineering Center, Davis, Calif.

United States Geological Survey (USGS). (2005). "USGS continues to analyze flooding effects from Hurricanes Frances and Ivan in Western North Carolina, 2004." ⟨http://nc.water.usgs.gov/info/news_release/floods04.html⟩ (Mar. 20, 2005).

Wang, Y., and Zheng, T. (2005). "Comparison of light detection and ranging and national elevation dataset digital elevation models on floodplains of North Carolina." *Nat. Hazards Rev.*, 6(1), 34–40.

Whol, E., and Oguchi, T. (2005). "Geographic information systems and mountain hazards." *Geographic information science and mountain geomorphology*, M. P. Bishop and J. F. Schroder Jr., eds., Springer, New York, 309–341.

Woolard, J. W., and Colby, J. D. (2002). "Spatial characterization, resolution, and volumetric change of coastal dunes using airborne LIDAR." *Geomorphology*, 48(1–3), 269–287.

Zerger, A. (2002). "Examining GIS decision utility for natural hazard risk modeling." *Environ. Modell. Software*, 17(3), 287–294.

Zerger, A., and Wealands, S. (2004). "Beyond modeling: Linking models with GIS for flood risk management." *Natural Hazards*, 33(2), 191–208.

Zhang, W., and Montgomery, D. R. (1994). "Digital elevation model grid size, landscape representation, and hydrologic simulations." *Water Resour. Res.*, 30(4), 1019–1028.